Ultrafast Relaxation Process of Excited-State NH_4 Radical in Ammonia Clusters

Nobuhiro Okai, Akihiro Takahata, Masayuki Morita, Shinji Nonose, and Kiyokazu Fuke*

Department of Chemistry, Faculty of Science, Kobe University, Nada-ku, Kobe 657-8501, Japan

Received: June 24, 2003; In Final Form: September 25, 2003

Relaxation process of ammoniated NH_4 radicals in the first excited state is studied with a femtosecond pump−probe technique and a time-of-flight mass spectroscopy. Small ammoniated NH_4 radicals are produced by an ArF-excimer laser photolysis of ammonia clusters. The decay of the excited state is probed by a resonance-enhanced two-photon ionization method. NH_4 radical in the first excited state is found to have a lifetime of an order of 50 ps. The lifetimes of $NH_4(NH_3)_n$ decrease from 1.4 ps ($n = 1$) to 300 fs ($n = 4$) with increasing the number of solvent molecules. The large reduction of the lifetimes is ascribed to the enhancement of nonradiative decay process as a result of the drastic change in the electronic structure of these clusters with the addition of ammonia molecules. For larger clusters ($n \geq 5$), the lifetime becomes almost constant at 120 fs. The observed size dependence of the lifetimes is discussed in relation to the formation of a one-center ion-pair state by the spontaneous ionization of NH_4 in ammonia clusters.

I. Introduction

NH_4 is a typical hypervalent Rydberg radical and has known to be the key intermediates in a resonance enhanced two-photon ionization (RE2PI) process of ammonia clusters through the first excited state.[1−5] Since the $A\ ^1A_2$-state ammonia is predissociative ($NH_3 \rightarrow NH_2 + H$, lifetime < 200 fs),[6,7] $NH_4(NH_3)_n$ are formed efficiently through an intracluster reaction. These clusters have substantially long lifetimes and are ionized by the second photon to form $NH_4^+(NH_3)_n$.[8−12] This process competes with the direct ionization of the excited-state $(NH_3)_n$* by the second photon, which is followed by proton-transfer reaction in the ionic state. Recently, these two mechanisms to produce $NH_4^+(NH_3)_n$ have been confirmed experimentally using the nanosecond[8,9] and femtosecond pump−probe techniques.[9−12] Since free NH_4 is unstable with respect to an H-atom dissociation and has a very short lifetime (13 ps),[9] most of spectroscopic studies have been carried out for ND_4.[1,13−15] Porter and co-workers have studied the stability of small $NH_4(NH_3)_n$ by a neutralized ion beam spectroscopy.[16,17] The lifetimes of these clusters have also been examined by two-step photoionization experiments with nano- and femtosecond lasers.[8−12,18−19] The structure and binding energy of ammoniated NH_4 clusters have also been investigated theoretically.[20−23]

The other interesting feature of NH_4 originates from its loosely bounded electron as in the case of alkali atoms. The existence of this radical has been speculated in solution, especially in the reaction of solvated electron and in electrochemistry.[24,25] If the radical exists in condensed phase, the Rydberg electron would be substantially influenced by solvent molecules and might be extensively diffused.[20−23] In relation to this issue, the electronic structure of the polar-solvent clusters containing alkali atoms has been investigated to model microscopic solvation of electrons and metal ions.[26−38] Vertical ionization energies of these clusters have been determined as a function of solvent molecules.[26−29] Photoelectron spectra of negatively charged alkali atom−solvent clusters such as $Li^-(NH_3)_n$ and $Na^-(NH_3)_n$ have also been examined to characterize the electronic structure of the alkali atoms in clusters.[29−35] Recently, the electronic absorption spectra of solvent clusters containing alkali atoms such as Na[36,37] and Li[38] have been measured. The geometric and electronic structures of these clusters have also been studied using various theoretical methods.[39−42] Both experimental and theoretical results indicate that the alkali metal atom is spontaneously ionized in small clusters to form a one-center ion-pair state. Since NH_4 is isoelectronic with an alkali atom, ammoniated NH_4 radicals are also interesting targets to explore the electron localization mode in clusters. In our previous works, the ionization potentials of $NH_4(NH_3)_n$ have been determined by photoionization threshold measurements.[43] We have also examined the photodepletion spectra of $NH_4(NH_3)_n$ ($n = 1−8$).[44,45] The spectra exhibit the drastic change in the electronic structure of NH_4 even in small clusters.

In the present work, the lifetimes of ammoniated NH_4 radicals are examined by the pump−probe technique with femtosecond laser pulses in order to get further insight into the electronic structure of the excited-state NH_4 in clusters. The lifetime of free NH_4 is determined to be longer than 50 ps, which is much shorter than the estimated radiative lifetime. With addition of a single ammonia molecule, the lifetime is reduced to 1.4 ps. For larger clusters, the lifetime decreases further to 120 fs. From comparison of these results with those for $Na(NH_3)_n$ reported in the literature,[46,47] the mechanism of the extensive enhancement for the nonradiative rates of $NH_4(NH_3)_n$ will be discussed.

II. Experimental Section

Details of the experimental apparatus used in the present study have been described elsewhere.[28,45] The system consists of a three-stage differentially evacuated chamber, which includes a cluster source and a reflection type time-of-flight (TOF) mass spectrometer.The ammonia (NH_3, minimum purity of 99.99%, Nippon Sanso) is used without further purification. Ammonia clusters are generated by a supersonic expansion of pure ammonia (4 atm) from a pulsed nozzle (General valve, series 9). Clusters containing NH_4 radicals, $NH_4(NH_3)_n$, are produced by the photolysis of ammonia clusters using an ArF excimer

* Author to whom correspondence should be addressed. Phone: 81+78 (803) 5673. Fax: 81+78 (803) 5673. E-mail: fuke@kobe-u.ac.jp.

10.1021/jp030784d CCC: $27.50
Published on Web 01/08/2004

laser (Lambda Physik COMPex 100) at 193 nm. Ammoniated NH_4 radicals generated via the intracluster reactions are detected by the resonance-enhanced two-photon ionization process with using the femtosecond pump and probe pulses.

Femtosecond laser pulses are generated by a Ti-sapphire laser (Spectra Physics, Tsunami). The output is amplified to ca. 1 mJ/pulse by a regenerative amplifier pumped by a 1 kHz YLF laser (Spectra Physics, Merline). The output is amplified further by a 10 Hz Nd:YAG laser (Quanta-Ray, GCR-150) to ca. 10 mJ/pulse. The pump pulses in the near-infrared region (1200−1800 nm) are generated by a home-built optical parametric amplifier (OPA). The two-stage β-BaB_2O_4 (BBO) OPA used is similar to that reported in ref 48. Nearly half of the output power of the regenerative amplifier is used for pumping OPA. A small portion of the amplified 800 nm pulses is focused into a sapphire plate to generate a white-light continuum. This radiation is amplified by two steps using a single type-II BBO crystal. Near-infrared pulses with pulse energy (sum of signal and idler) of about 300 μJ is generated across the whole tuning range. Since the absorption band positions of $NH_4(NH_3)_n$ change drastically with n as mentioned later, we use various combinations of the pump and probe wavelengths. For example, the pump and probe pulses at 1250 (ca. 50 μJ/pulse) and 400 nm (ca. 200 μJ/pulse), respectively, are used for the lifetime measurement of $NH_4(NH_3)_2$. The duration time of the pump pulse is measured by up-conversion with the pulse at the fundamental. The cross-correlation trace at the signal wavelength of 1250 nm gives a full width at half-maximum (fwhm) of about 330 fs. Assuming a $sech^2$ pulse, the deconvolution leads to a width of the pump pulse of 210 fs. The second harmonic at 400 nm is used as the probe pulses. The pump pulse from OPA and the probe pulse passed through a delay stage are recombined using a 45° high reflector. These laser pulses and the photolysis laser beam are introduced counterpropergatedly to an acceleration region of the mass spectrometer without focusing, where they intersect with the cluster beam. Cluster ions produced by two femtosecond pulses are accelerated and introduced to a field-free region of the reflectron TOF mass spectrometer. The ions are reflected by electric fields at the end of the TOF chamber and are detected by dual microchannel plates (Hamamatsu, F1552-23S) after flying back into the field-free region. The output signals are fed into a digital storage oscilloscope (LeCroy 9450) after being amplified by a wide-band amplifier (NF Electronic Instruments, BX-31). The mass spectra are measured at various delay times between the pump and probe pulses. The decay time profiles are obtained by plotting the ion signals in the mass spectra as a function of the delay time.

Figure 1 shows a typical mass spectrum of $NH_4^+(NH_3)_n$ produced by the resonance-enhanced two-photon ionization (RE2PI) process via the *A* state by irradiating the ArF laser and two femtosecond laser pulses. The photolysis is carried out at 2 mm upstream from the ionization region, where the pump and probe pulses are introduced with a delay time of 2 μs. Since the lifetimes of $NH_4(NH_3)_n$ ($n \geq 1$) are longer than a few microseconds,[45] enough RE2PI signals can be detected even ionizing the clusters at 2 mm downstream. As indicated in this figure, each cluster exhibits two peaks with the 2-μs delay time. In the RE2PI, two processes such as an absorption−dissociation−ionization (ADI) and an absorption−ionization−dissociation (AID) have been observed for the production of $NH_4^+(NH_3)_n$.[45] The mass peaks that appeared at an earlier time correspond to the ion signals produced through the AID process with two photons of the ArF laser, while the second peaks with the 2-μs delay time are the ADI signals, which are generated by the ionization of $NH_4(NH_3)_n$ formed through the photolysis of ammonia clusters. Thus, the lifetime of the excited-state $NH_4(NH_3)_n$ ($n \geq 1$) is examined at 2 mm downstream from the ArF laser beam. With this scheme, we can avoid the superposition of the strong AID signals and can detect the pump−probe signal with a good S/N ratio. Unfortunately, we cannot use the same scheme for the lifetime measurement of a short-lived NH_4, and thus, we use a more tedious method as mentioned later. The decay time profile is recorded by monitoring the cluster ion signals as a function of the delay time between the pump and probe laser pulses.

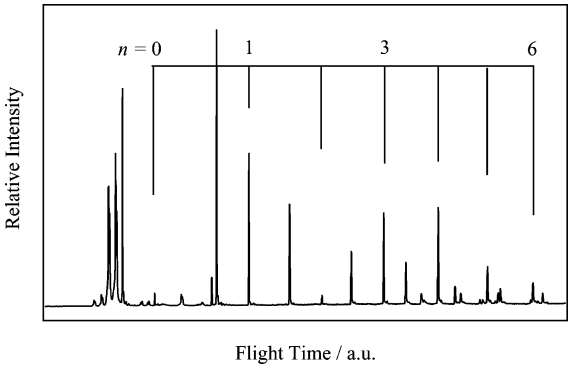

Figure 1. Typical TOF mass spectrum of $NH_4^+(NH_3)_n$ produced by RE2PI via the A state by irradiating the ArF laser and two femtosecond pulses. The delay time between the photolysis (193 nm) and the pump−probe (800 and 400 nm) lasers is 2 μs. Each cluster exhibits two peaks corresponding to the AID and ADI processes.

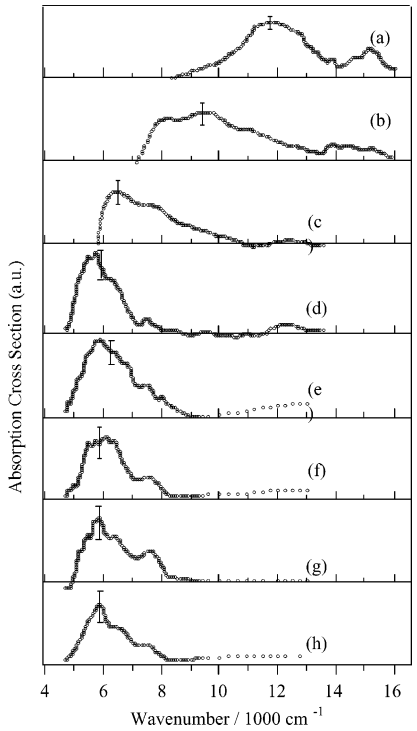

Figure 2. Low-resolution absorption spectra of $NH_4(NH_3)_n$ ($n = 1$ (a) to 8 (h)) in the energy region of 4500−16 000 cm^{-1}. These spectra are cited from ref 45.

III. Results and Discussion

Figure 2 shows the low-resolution absorption spectra of $NH_4(NH_3)_n$ in the energy region of 4500−16000 cm^{-1} cited from ref 45. The electronic states of these clusters have been discussed in the previous paper, and therefore the results are briefly summarized here to make the discussion clear in the following

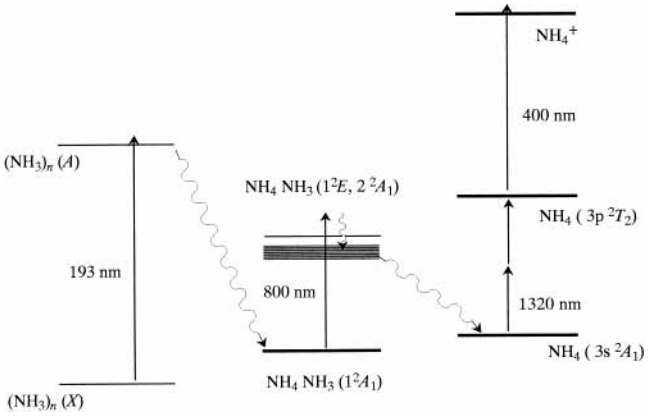

Figure 3. Scheme of the pump−probe experiment for free NH_4. To avoid the strong ion signals generated by the first photolysis at 193 nm, the pump−probe experiment is carried out for NH_4 produced by the second photolysis of NH_4NH_3 at 800 nm.

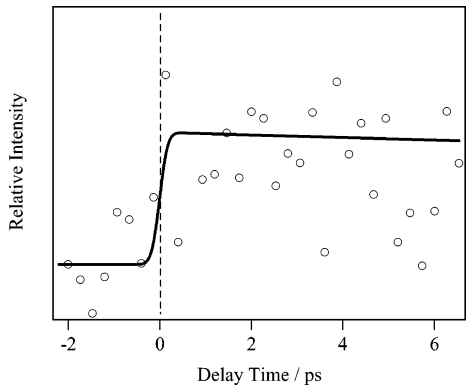

Figure 4. Pump−probe data of NH_4^+ with the pump pulses at 1320 nm and the probe pulses at 400 nm. The solid curve is the best fit to a single-exponential decay function.

paragraphs. Since free NH_4 is short-lived, the $3p\ ^2T_2-3s\ ^2A_1$ transition of this radical in the visible region has been studied by emission spectroscopy and its band origin is located at 15062 cm^{-1}.[1] In ammonia clusters, this transition is shifted to the red as in the case of the isoelectronic systems such as $Li(NH_3)_n$[29,30] and $Na(NH_3)_n$.[30,36,37] From the comparison with the results of $Li(NH_3)_n$, the observed bands of $NH_4(NH_3)_n$ in Figure 2 have been assigned to those derived from the 3p−3s transition of NH_4. For the 1:1 complex, we have recorded the vibrationally resolved spectrum, which exhibits two vibronic transitions starting at 9305 ± 15 and 10 073 ± 15 cm^{-1}. On the basis of the theoretical results of the geometry and electronic structure for the complex, we have assigned these origins to those of the $2\ ^2A_1$ (z) and $1\ ^2E$ (x,y) excited states derived from the $3p\ ^2T_2$ state of NH_4.

The 3p−3s-type transition of $NH_4(NH_3)_2$ exhibits a broad and blue-shaded maximum at about 9000 cm^{-1} which is shifted by about 2500 cm^{-1} from $n = 1$ with addition of the second NH_3. The large spectral shift indicates that the second NH_3 also binds directly to NH_4 as predicted by the theoretical calculations.[20,21,23] The spectra of $NH_4(NH_3)_3$ and $NH_4(NH_3)_4$ in Figures 2c and 2d exhibit the strong peaks at ∼6500 and ∼5800 cm^{-1}, respectively, showing a sudden decrease in bandwidth from $n = 3$ to 4. The spectral change has been interrelated in terms of the filling of the first solvation shell with four ammonia molecules. The theoretical calculations predict that $NH_4(NH_3)_4$ has the T_d structure, in which four NH_3 molecules are directly bound to NH_4 through hydrogen bonds.[20,23] In this symmetry, the 3p orbitals of NH_4 interact equivalently with four NH_3 molecules and the splitting of the excited states becomes much smaller. The absorption spectra for $n \geq 5$ in Figures 2e−2h show a rather sharp bandwidth and no appreciable change in band position from that of $n = 4$. The extensive red-shift of these clusters ($n \leq 4$) has been ascribed to the change in the electronic structure from the localized one to those delocalized over the solvent molecules.

As mentioned previously, the lifetime of NH_4 in the ground state ($3s\ ^2A_1$) is very short (13 ps),[9] and thus, it is difficult to measure the decay time with the method used for larger clusters mentioned later. To avoid the superposition of the strong AID signal of the ArF laser, we carry out the lifetime measurement for NH_4 ($3p\ ^2T_2$) with using the scheme shown in Figure 3: NH_4 generated through the photodecomposition of the 1:1 complex in the ionization region of the mass spectrometer is used as the sample. NH_4NH_3 has the strong absorption at 800 nm as seen in Figure 2 and the excited-state complex decomposes within a few picoseconds as shown later. The fundamental of the Ti-sapphire laser used as the second photolysis laser is introduced at 2 mm downstream from the ArF laser with a delay time of 2 μs. NH_4NH_3 generated by the photolysis drifts downstream and is decomposed by the irradiation of the 800-nm pulses to form NH_4. Free NH_4 thus produced in molecular beams is promoted to the first excited state with two photons of the 1320-nm pump pulse, and then, it is ionized with the probe pulse at 400 nm; two laser beams are introduced collinearly with the 800-nm laser beam. Figure 4 shows the decay time profile of NH_4 recorded as a function of the delay time between the 1320- and 400-nm pulses. Since NH_4 is formed through the two-step photolysis as mentioned above, the signal-to-noise ratio is rather poor. The fit of the decay curve of NH_4 ($3p\ ^2T_2$) gives the lower limit of the lifetime as about 50 ps.

The excited-state lifetimes of NH_4 and ND_4 have also been examined by Ketterle et al. using a neutralized ion beam technique.[49] In this experiment, the excited-state radicals are generated through the charge recombination in a charge exchange cell, which is crossed with a molecular beam of ammonium ions. The lifetime of the excited-state radicals has been measured by monitoring the light emission of the Schüler band as a function of the position of the cell; the lifetime of ND_4 ($3p\ ^2T_2$) has been determined to be 4.2 ns. They have also tried to measure the lifetime of NH_4 and observed the light emission identified as the Schüler band at 663.37 and 663.68 nm. However, the observed emission intensity of NH_4 is an order of magnitude weaker than that of ND_4, indicating the lifetime of less than 500 ps. These results suggest that the lifetime of NH_4 estimated in the present work may give a lower limit (about 50 ps). This number is significantly smaller than the radiative lifetime (15 ns) calculated from the transition dipole moment and the experimental transition energy.[49] The result also indicates the large deuterium isotope effect. Two possible mechanisms such as the direct dissociation and the predissociation via nonradiative transition to the ground state can be considered to explain the large isotope effect on the decay of NH_4. The potential energy surfaces of the ground and low-lying excited states of NH_4 have been extensively studied by several theoretical groups.[20,50−54] The adiabatic potential curves along the $NH_3 + H$ and $NH_2 + H_2$ dissociation coordinates are schematically shown in Figure 5. The radical in the ground state has known to have a very shallow well of about 0.7 eV along the NH_3+H dissociation coordinate.[50,52,53] In the first excited state, NH_4 is strongly bound along this coordinate and no direct dissociation channel would be expected. In addition to this channel, NH_4 has another dissociation channels to produce NH_2 both in the ground ($1\ ^2B_1$) and first excited ($1\ ^2A_1$) states. The

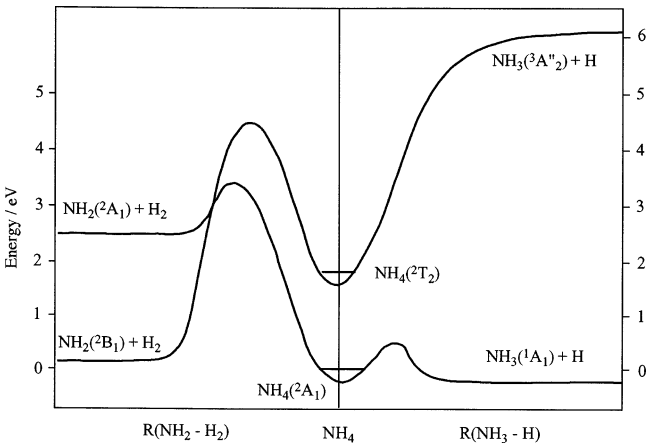

Figure 5. Schematic potential energy curves for free NH_4 along the $NH_2 + H_2$ and $NH_3 + H$ dissociation coordinates. The energies of the potential well depths, barrier heights, and the asymptotes are cited from refs 53 and 54.

details of the potential energy surfaces for these channels have been investigated theoretically.[52,54] The ground $^2A_1$ state of NH_4 correlates to the ($NH_2(1\ ^2A_1) + H_2$) asymptote. There exists an energy barrier along this reaction coordinate, which arises from an avoided curve crossing between the repulsive state of the Rydberg radical ((NH_4^+)(e)3s) and the state arising from an antibonding interaction of the ($NH_2(1\ ^2A_1) + H_2$) asymptote. The energy barrier heights of $^2A_1$ from the transition state to NH_4 and ($NH_2(1\ ^2A_1) + H_2$) are ≈3.59 and 1.06 eV, respectively. On the other hand, the first excited $^2T_2$ state correlates adiabatically to the ground state of NH_2 (($NH_2(1\ ^2B_1) + H_2$) asymptote). Along this coordinate, there exists a similar energy barrier resulting from an avoided curve crossing of the repulsive state of NH_4 and the state emerging from the ($NH_2(1\ ^2B_1) + H_2$) asymptote. The energy barrier heights of $^2B_1$ from the transition state to NH_4 and ($NH_2(1\ ^2B_1) + H_2$) are ≈2.96 and 4.66 eV, respectively. These theoretical results indicate that the dissociation into ($NH_2 + H_2$) is endothermic (−2.53 eV) in the ground state and does not contribute to the decay of $NH_4(1\ ^2A_1)$. The situation would be different in the excited-state NH_4 because the dissociation is exothermic though the energy barrier is rather high. The excited-state NH_4 radicals produced by the charge recombination in the neutralized ion beam experiment may be quite hot and, to some extent, the nascent radicals decay through the direct dissociation channel via tunneling. On the other hand, in the present experiment, the radicals are generated by the photolysis of the 1:1 complex in the collision-free condition. And thus, the nascent NH_4 radicals internally excited are promoted to the electronically excited state by the irradiation of the pump laser with holding the internal excitation energy. However, the potential well depth of the ground state is calculated to be rather shallow (0.75 eV)[53] and the internally hot radicals may decompose within a short time. As a result, the effective barrier height becomes higher compared with the NH_4 radicals produced in the neutralized ion beam experiment. Thus, these theoretical results suggest that the direct dissociation channel would be not so important in the present experiment.

The other possible origin for the large isotope effect observed for the lifetimes of NH_4 and ND_4 is the nonradiative transition followed by the predissociation to $NH_3 + H$ on the ground-state surface. The nonradiative transition process for organic molecules has been studied extensively in the condensed phase.[55] For example, a strong isotope effect has been observed in the intersystem crossing process ($T_1 \rightarrow S_0$) of aromatic compounds; the rates for perhydro-aromatic hydrocarbons are an order of magnitude faster than those for perdeutero-compounds. And also, the rate has found to depend exponentially on the energy gap between the initial and final states of nonradiative transition. In the earlier studies, these observations have been extensively discussed and the "golden rule" rate expression has been proposed for the thermally averaged rates as follows:[55]

$$k_{nr}(i \rightarrow f) = \frac{2\pi}{\hbar}\beta_{if}^{\ 2}\sum_n |\langle m_i|n_f\rangle|^2 \rho_{fn}(E_{if}) \qquad (1)$$

where $k_{nr}(i \rightarrow f)$ and β_{if} are the nonradiative decay rate and nonadiabatic interaction matrix element between the initial and final electronic states, respectively. $\langle m_i|n_f\rangle$ and $\rho_{fn}(E_{if})$ are the thermal averaged Franck−Condon factor between the initial and final vibrational levels such as $\langle im|$ and $|fn\rangle$, and the effective density of states for $|fn\rangle$, respectively. The analytical expressions of nonradiative rate for large molecules have also been derived for a simple displaced potential surface model with the harmonic approximation using a generating function method.[56] This study has established the energy gap law for the observed exponential dependence of the nonradiative decay rate. The theory has also confirmed the previous predictions that the most effective accepting modes are those of the highest frequency modes and the observed isotope effect is determined by the high-frequency C−H (or C−D) stretching modes. As in the case of aromatic compounds, the highest-frequency vibrational modes of NH_4 such as the symmetric (ν_1, a_1) and antisymmetric (ν_3, t_2) stretching modes are expected to become the accepting modes; the calculated frequencies are 3092 and 3176 cm^{-1}, respectively.[54] These arguments are consistent with the observed strong isotope effect. Although the density of states is considerably larger in ND_4 than in NH_4, the Franck−Condon factors are much smaller in the former case. Thus, the difference in the Franck−Condon factors may lead to the observed isotope effect.

For NH_4NH_3, the $1\ ^2T_2$ state of NH_4 was found to split into two low-lying excited states such as the $2\ ^2A_1$ and $1\ ^2E$ states in C_{3v} symmetry. The origins of these excited states are located at 9300 and 10 500 cm^{-1} for the $2\ ^2A_1$ and $1\ ^2E$ states, respectively. Unfortunately, the laser pulses at this photon energy are difficult to generate with enough intensity using the Ti-sapphire laser system, and thus, we use the fundamental and second harmonic as the pump and probe pulses, respectively. Figures 6a and 6b show the decay time profiles for the 1:1 complex produced with the pump pulses at 790 and 840 nm, respectively. Since the lifetime of the ground-state NH_4NH_3 is rather long (3 μs), the delay time between the photolysis and pump lasers is set at about 2 μs to avoid the strong AID signal of the photolysis laser as seen in Figure 1. The decay curves in Figure 6 are fitted to a single-exponential function and give the lifetimes of 1.5 and 1.4 ps for the 790- and 840-nm excitations, respectively. In two excitations, the excess energies above the origin of the 2^2A_1 state are 3360 and 2600 cm^{-1}, respectively. These results indicate that the lifetimes may not be dependent on the excess vibrational energy; the internal conversion to the ground state in this energy region may be much faster than the rate of intramolecular vibrational relaxation. Although the radiative rate may also change with the excitation energy, this factor may be neglected because the rate is expected to decrease with decreasing by third power of the excitation energy based on the transition-probability argument. Thus, the reduction of the lifetime by more than two orders with addition of an ammonia molecule is ascribed to the large enhancement of nonradiative process. In relation to these observation, recently, Schultz and co-workers have measured the excited-state lifetimes

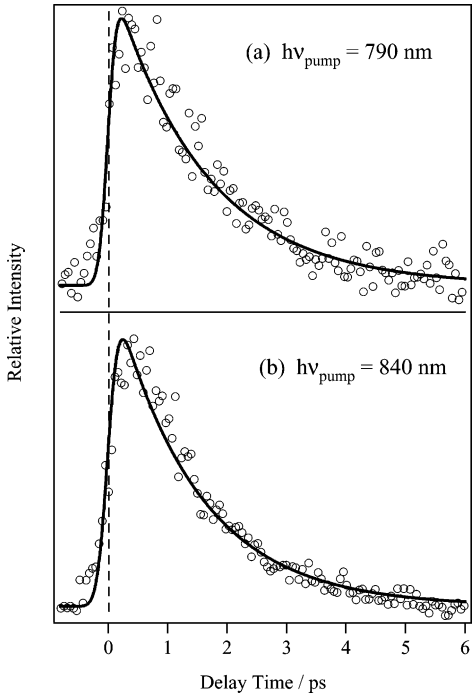

Figure 6. (a) Pump−probe data of $NH_4NH_3^+$ with the pump and probe pulses at 790 nm and 395 nm, respectively. Curve (b) for $NH_4NH_3^+$ with pump pulses at 840 nm and probe pulses at 420 nm. The solid curves are the best fits to a single-exponential decay function.

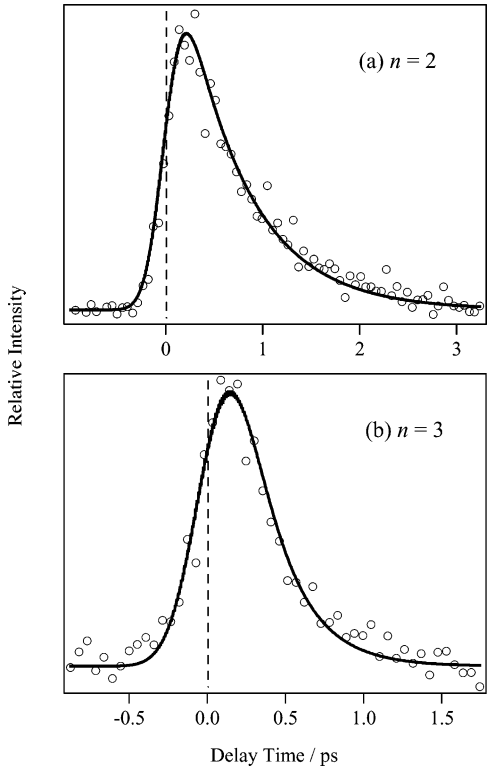

Figure 7. Pump−probe data for $n = 2$ (a) and $n = 3$ (b). Curve (a) is recorded with the pump and probe pulses at 1250 (60 μJ/cm^2) and 395 nm (200 μJ/cm^2), respectively. Curve (b) is recorded with the pump and probe pulses at 1550 (90 μJ/cm^2) and 790 nm (810 μJ/cm^2), respectively. The solid curves are the best fits to a single exponential decay function.

of $Na(NH_3)_n$ using the similar pump−probe technique.[46,47] They have determined the lifetimes of $NaNH_3$ and $NaND_3$ as 1.1 and 5 ns, which are much shorter than the radiative lifetime of the Na atom (11 ns). Interestingly, the rate of the nonradiative transition for the $NH_4(NH_3)$ complex (6.6×10^{11} s^{-1}) is much faster than that for $NaNH_3$ (8.2×10^8 s^{-1}). Although many efforts have been made for the calculations of the nonradiative transition rate, those are limited for the weak coupling systems.[55] In the case of NH_4NH_3, the situation is different. As mentioned previously, the excitation energy of the first excited (2^2A_1) state of NH_4NH_3 is shifted to the red by 5760 cm^{-1} from that of NH_4. This number gives the binding energy of the 2^2A_1 state as 0.98 eV, which is much larger than that of the ground state (0.34 eV) and is almost the same as that for the cation complex (1.06 eV). Thus, the complex in the excited state has the ionic character close to the ionic state, $NH_4^+NH_3$, with a loosely bounded electron. The extensive changes in the geometrical and electronic structures for the low-lying states of NH_4NH_3 make a quantitative analysis of the nonradiative transition very difficult. In addition, the internal conversion process may also include an H-atom transfer through tunneling process. Therefore, a sophisticated quantum mechanical molecular dynamics calculation may be necessary to estimate the nonradiative rate constant. At the moment, we cannot calculate the rate explicitly; however, the large enhancement of the nonradiative process for NH_4NH_3 compared with that for $NaNH_3$ may be safely ascribed to the presence of the high-frequency accepting mode such as the N−H stretching vibration as in the case of aromatic molecules.

As seen in Figure 2, the absorption spectra of $NH_4(NH_3)_2$ and $NH_4(NH_3)_3$ also exhibit large red-shifts; the absorption peaks are observed at 8000 and 6500 cm^{-1} for $n = 2$ and 3, respectively. According to the theoretical calculations, the second and third ammonia molecules are directly bound to NH_4 through the N−H hydrogen bonds, and as a result, the electronic structure of NH_4 in these clusters is significantly altered. These theoretical predictions are consistent with the further change in the absorption bands for these clusters. The lifetimes of $n = 2$ and 3 become much shorter as seen in Figure 7. The decay curve of $n = 2$ is obtained by RE2PI process with the pump and probe pulses at 1250 (60 μJ/cm^2) and 395 nm (200 μJ/cm^2), respectively. On the other hand, the decay curve of $n = 3$ (b) is measured by (1 + 2) REMPI with the pump and probe pulses at 1550 (90 μJ/cm^2) and 790 nm (810 μJ/cm^2), respectively. The results of fittings give the decay time of 650 and 250 fs for $n = 2$ and 3, respectively. These clusters exhibit the large red-shift as mentioned above and the reduction of the lifetime may be consistent with the energy gap law. With addition of the fourth ammonia molecule, the absorption peak slightly shifts to the red and the bandwidth becomes much narrower. In our previous paper, these spectral changes have been ascribed to the filling of the first solvation shell, in which four ammonia molecules directly bound to NH_4 with T_d symmetry. The increase in symmetry both in the ground and excited states would significantly reduce the geometrical change in the electronic transition. A careful measurement of the lifetime of $NH_4(NH_3)_4$ (300 fs) indicates that the nonradiative decay rate of this cluster is slightly slower than that for $n = 3$ (250 fs) as seen in Figures 8 and 9. Similar slowing of the decay rate has also been observed for $Na(NH_3)_4$ as shown in Figure 9, which also has the T_d geometry.[46,47] In both systems, the $n = 4$ clusters have the lowest excitation energy among the clusters and may have the largest decay rate if the energy gap law is valid. The observed slowing in the decay rate suggests that the simple energy gap law does not hold in these clusters.

For the larger clusters with $n > 4$, the decay time profiles are measured with the pump and probe pulses at 1550 and 530 nm, respectively. The lifetimes of $NH_4(NH_3)_n$ decrease further as seen in Figure 8; the results of fittings give the decay time

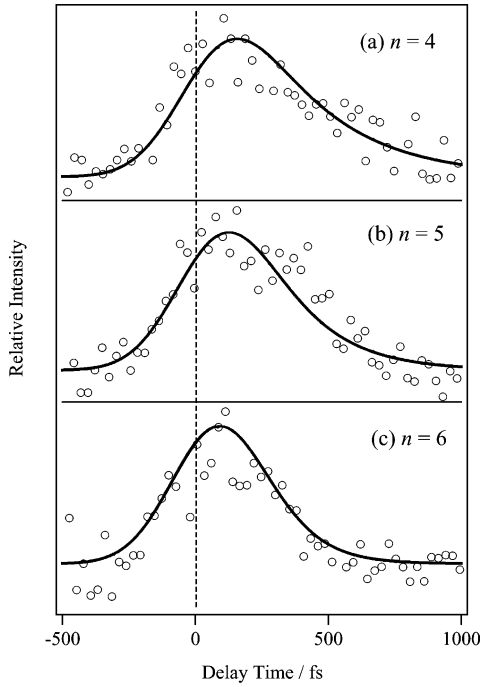

Figure 8. Pump−probe data for $n = 4$ (a), $n = 5$ (b), and $n = 6$ (c). These decay curves are recorded by (1 + 1) RE2PI with the pump and probe pulses at 1550 (60 μJ/cm^2) and 530 nm (55 μJ/cm^2), respectively. The solid curves are the best fits to a single-exponential decay function.

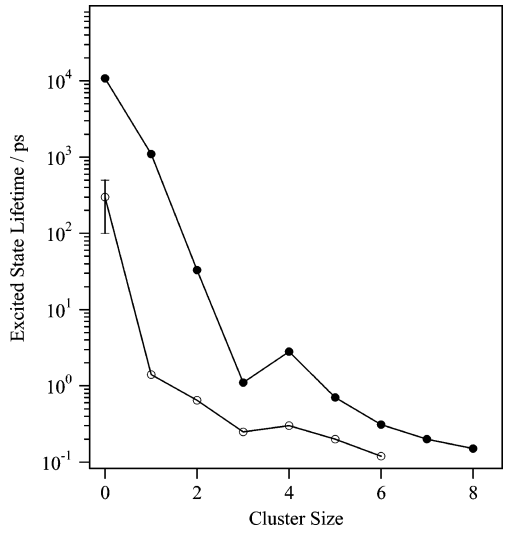

Figure 9. Lifetimes of $NH_4(NH_3)_n$ ($n = 0-6$) (○) plotted as a function of cluster size. For comparison, the results for $Na(NH_3)_n$ ($n = 0-8$) (●) in ref 47 are also plotted.

of 200 and 120 fs for $n = 5$ and 6, respectively. These results indicate that the lifetimes seem to become constant at 120 fs, which is close to those for Na $(NH_3)_n$ ($n > 5$) as shown in Figure 9. This trend in the lifetimes seems to be coherent with that in the absorption spectra. The spectra for the larger clusters in Figure 2 slightly shift back to the blue. A similar spectral change has also been found in the absorption spectra of $Na(NH_3)_n$ ($n \geq 5$). Moreover, the photoelectron spectra (PES) of negatively charged $Li^-(NH_3)_n$ and $Na^-(NH_3)_n$ reported previously by our group also exhibit similar spectral trends.[29,30] In the PES, photodetachment transitions to the neutral ground and low-lying excited states derived from the ^{2}S and ^{2}P-type levels of alkali atoms are observed. The spectra of $Li^-(NH_3)_n$ and $Na^-(NH_3)_n$ exhibit a rapid decrease in the energy separation between the ground and first excited states, being consistent with the large red-shift of the $^2P-^2S$ type transition in the absorption spectra of $Na(NH_3)_n$. To explain the extensive change in the electronic structure of the metal atoms in small clusters, the radial distribution (RD) for the unpaired electron of $Na(NH_3)_n$ ($n = 0-4$) at their anionic geometries has been calculated for the isomers with the structures having as many Na−N bonds as possible for each n. Both in the ground and first excited states, the R_{max} values, defined as the maximum RD, have found to increase with increasing n. For $n = 4$, the R_{max} values for the 3^2S- and 3^2P-type states become about 2.0 and 1.7 times greater than the corresponding atomic values; the unpaired electron is diffused by ammoniation not only in the ground state but also in the excited state. These changes in the electronic structure of neutral clusters correspond to the change from the atomic-like to the one-center ion-pair state. From the comparison with these theoretical results, the rapid decrease in the $^2P-^2S$ energy separation of solvated alkali metal atom has been ascribed to the spontaneous ionization of the metal atom in clusters.[25,26,33] As mentioned previously, the size dependences of the absorption spectra for $NH_4(NH_3)_n$ and $Na(NH_3)_n$ are very similar to each other. Similar size dependence has also been observed for the ionization potentials (IPs) of $NH_4(NH_3)_n$[43] and $M(NH_3)_n$ (M = Li,[57] Na,[58] and Cs[59]). For $NH_4(NH_3)_n$, the IPs have been found to decrease monotonically with increasing n to a limit of 1.33 eV, which coincides with the limits (1.40 eV) for $M(NH_3)_n$ (M = Li, Na, and Cs) as well as the photoemission threshold of liquid NH_3. These observations strongly suggest that the NH_4 radical is ionized in small ammonia clusters to form the one-center ion-pair state as in the case of the alkali atom−ammonia systems. This prediction has been confirmed theoretically by Hashimoto and co-workers.[25] They have examined the spatial distribution of the unpaired electron for $NH_4(NH_3)_n$ ($n \leq 4$) using the ab initio MO method at the contracted level. From these calculations, the observed large spectral red-shift and the successive decrease in the ionization energies have been ascribed to the growing one-center Rydberg nature of $NH_4(NH_3)_n$ as in the case of the alkali atom−ammonia system; the Rydberg electron is squeezed out over the ammonia molecules when the first solvation shell is closed. These experimental and theoretical results clearly indicate that the relevant orbitals involved in the electronic transition are delocalized over the solvent molecules and the electronic excitation is no longer localized on NH_4 and Na atom. Owing to the diffused electronic structures of these clusters, the electronic relaxation process becomes similar to each other and depends strongly on the interaction between the valence electron and ammonia molecules. As seen in Figure 9, the lifetimes of $NH_4(NH_3)_n$ and $Na(NH_3)_n$ become almost constant at about 100 fs. This trend seems to be consistent with the above arguments on the delocalization of unpaired electrons. It is worth noticing that the ion-pair state mentioned above is considered to be a precursor of the solvated electron in liquid ammonia. If this is the case, the observed decay ($3p \rightarrow 3s$) process may correspond to a final step in the cooling process of a trapped solvated electron. Recently, Unterreiner and co-workers[60] have performed the femtosecond near-infrared pump−probe experiments of an equilibrated solvated electron in liquid ammonia. They have ascribed the observed transient to the absorption of hot electrons generated through the photoexcitation process and determined the time scale of the excited-state relaxation as 100 fs, which is very close to the lifetimes of $NH_4(NH_3)_n$ and $Na(NH_3)_n$ ($n \geq 5$). To compare the present results with the decay rate in liquid ammonia, we are carrying out transient absorption experiments for NH_4 in liquid ammonia.

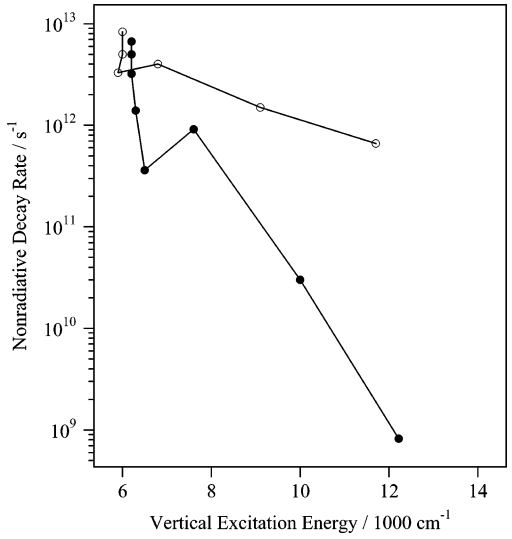

Figure 10. Nonradiative decay rates of $NH_4(NH_3)_n$ ($n = 1-6$) (○) plotted as a function of the vertical excitation energy of the first excited state. For comparison, we also plot the results for $Na(NH_3)_n$ ($n = 1-8$) (●), which has been reported in ref 47.

Figure 10 shows the summary of the estimated nonradiative decay rate for $NH_4(NH_3)_n$ and $Na(NH_3)_n$ ($n = 1-6$) from the observed lifetimes. We plot the data as a function of the vertical excitation energy to examine the validity of the energy gap law. The results exhibit to some extent a correlation behavior. However, because of the limited data, it is difficult to discuss further the size effect quantitatively.

Acknowledgment. This work is partially supported by the Grant-in-Aid (Grants 11304042 and 15035209) from the Ministry of Education, Science, Sports and Culture of Japan and a JSPS research grant for the Future Program. K.F. is also grateful to the Japan Science Foundation and the Hyogo Science and Technology Association for partial financial support.

References and Notes

(1) Herzberg, G. *Faraday Discuss. Chem. Soc.* **1981**, *71*, 165.
(2) Cao, H. Z.; Evleth, E. M.; Kassab, E. *J. Chem. Phys.* **1984**, *81*, 1512.
(3) Misaizu, F.; Houston, P. L.; Nishi, N.; Shinohara, H.; Kondow, T.; Kinoshita, M. *J. Phys. Chem.* **1989**, *93*, 7041.
(4) Wei, S.; Purnell, J.; Buzza, S. A.; Stanley, R. J.; Castleman, A. W., Jr. *J. Chem. Phys.* **1992**, *97*, 9480.
(5) Hertel, I. V.; Hüglin, C.; Nitsch, C.; Schultz, C. P. *Phys. Rev. Lett.* **1991**, *67*, 1767.
(6) Biesner, J.; Schnieder, L.; Schmeer, J.; Ahlers, G.; Xie, X.-X.; Welge, K. H.; Ashfold, M. N. R.; Dixon, R. N. *J. Chem. Phys.* **1988**, *88*, 3607.
(7) Fuke, K.; Yamada, H.; Yoshida, Y.; Kaya, K. *J. Chem. Phys.* **1988**, *88*, 5238.
(8) Misaizu, F.; Houston, P. L.; Nishi, N.; Shinohara, H.; Kondow, T.; Kinoshita, M. *J. Chem. Phys.* **1993**, 98, 336.
(9) Fuke, K.; Takasu, R. *Bull. Chem. Soc. Jpn.* **1995**, *68*, 3309.
(10) Wei, S.; Purnell, J.; Buzza, S. A.; Castleman, A. W., Jr. *J. Chem. Phys.* **1993**, *99*, 755.
(11) Purnell, J.; Wei, S.; Buzza, S. A.; Castleman, A. W., Jr. *J. Phys. Chem.* **1993**, *97*, 12530.
(12) Freudenberg, Th.; Radloff, W.; Ritze, H.-H.; Stert, V.; Weyers, K.; Noack, F.; Hertel, I. V. *Z. Phys. D* **1996**, *36*, 349.
(13) Whittaker, E. A.; Sullivan, B. J.; Bjorklund, G. C.; Wendt, H. R.; Hunziker, H. E. *J. Chem. Phys.* **1984**, *80*, 961.
(14) Watson, J. K. G. *J. Mol. Phys.* **1984**, *107*, 124.
(15) Alberti, F.; Huber, K. P.; Watson, J. K. G. *J. Mol. Phys.* **1984**, *107*, 133.
(16) Gellene, G. I.; Cleary, D. A.; Porter, R. F. *J. Chem. Phys.* **1982**, *77*, 3471.
(17) Jeon, S. J.; Raksit, A. B.; Gellene, G. I.; Porter, R. F. *J. Am. Chem. Soc.* **1985**, *107*, 4129.
(18) Snyder, E. M.; Castleman, A. W., Jr. *J. Chem. Phys.* **1997**, *107*, 744.
(19) Farmanara, P.; Radloff, W.; Stert, V.; Ritze, H.-H.; Hertel, I. V. *J. Chem. Phys.* **1999**, *111*, 633.
(20) Wan, J. K. S. *J. Chem. Educ.* **1968**, *45*, 40.
(21) Kariv-Miller, E.; Nanjundiah, C.; Eaton, J.; Swenson, K. E. *J. Elctroanal. Chem.* **1984**, *167*, 141.
(22) Kassab, E.; Evleth, E. M. *J. Am. Chem. Soc.* **1987**, *109*, 1653.
(23) Evleth, E. M.; Kassab, E. *Pure Appl. Chem.* **1988**, *60*, 209.
(24) Park, J. K.; Iwata, S. *J. Phys. Chem. A* **1997**, *101*, 3613.
(25) Daigoku, K.; Miura, N.; Hashimoto, K. *Chem. Phys. Lett*. **2001**, *346*, 81.
(26) Schulz, C. P.; Haugstatter, R.; Tittes, H.-U.; Hertel, I. V. *Z. Phys. D* **1988**, *10*, 279.
(27) Hertel, I. V.; Huglen, C.; Nitsch, C.; Schulz, C. P. *Phys. Rev. Lett*. **1992**, *67*, 1767.
(28) Misaizu, F.; Tsukamoto, K.; Sanekata, M.; Fuke, K. *Chem. Phys. Lett*. **1992**, *188*, 241.
(29) Takasu, R.; Hashimoto, K.; Fuke, K. *Chem. Phys. Lett*. **1996**, *258*, 94.
(30) Takasu, R.; Misaizu, F.; Hashimoto, K.; Fuke, K. *J. Phys. Chem. A* **1997**, *101*, 3078.
(31) Takasu, R.; Taguchi, T.; Hashimoto, K.; Fuke, K. *Chem. Phys. Lett*. **1998**, *290*, 481.
(32) Takasu, R.; Ito, H.; Nishikawa, K.; Hashimoto, K.; Okuda, R.; Fuke, K. *J. Electron Spectrosc. Relat. Phenom*. **2000**, *106*, 127.
(33) Misaizu, F.; Tsukamoto, K.; Sanekata, M.; Fuke, K. *Surf. Rev. Lett*. **1996**, *3*, 405.
(34) Fuke, K.; Hashimoto, K.; Iwata, S. *Adv. Chem. Phys.* **1999**, *110*, 431. Fuke, K.; Hashimoto, K.; Takasu, R. In *Advances in Metal and Semiconductor Clusters*; Duncan, M. A., Ed.; JAI Press Inc.: Amsterdam, 2000; Vol. 5.
(35) Takasu, R.; Hashimoto, K.; Okuda, R.; Fuke, K. *J. Phys. Chem. A* **1999**, *103*, 349.
(36) Schulz, C. P.; Nitsch, C. *J. Chem. Phys*. **1997**, *107*, 9794.
(37) Brockhaus, P.; Hertel, I. V.; Schulz, C. P. *J. Chem. Phys*. **1999**, *110*, 393.
(38) Takasu, R.; Nishikawa, K.; Miura, N.; Sabu, A.; Hashimoto, K.; Schulz, C. P.; Hertel, I. V.; Fuke, K. *J. Phys. Chem. A* **2001**, *105*, 6602.
(39) Hashimoto, K.; Kamimoto, T.; Fuke, K. *Chem. Phys. Lett*. **1997**, *266*, 7.
(40) Hashimoto, K.; Morokuma, K. *J. Am. Chem. Soc*. **1994**, *116*, 11436.
(41) Glendening, E. D. *J. Am. Chem. Soc*. **1996**, *118*, 2473.
(42) Combariza, J. E.; Kestner, N. R.; Jortner, J. *J. Chem. Phys*. **1994**, *100*, 2851.
(43) Fuke, K.; Takasu, R.; Misaizu, F. *Chem. Phys. Lett.* **1994**, *229*, 597.
(44) Nonose, S.; Taguchi, T.; Mizuma, K.; Fuke, K. *Eur. Phys. J. D* **1999**, *9*, 309.
(45) Nonose, S.; Taguchi, T.; Chen, F.; Iwata, S.; Fuke, K. *J. Phys. Chem. A* **2002**, *106*, 5242.
(46) Schulz, C. P.; Hohndorf, J.; Brockhaus, P.; Noack, F.; Hertel, I. V. *Chem. Phys. Lett.* **1995**, *239*, 18.
(47) Schulz, C. P.; Scholz, A.; Hertel, I. V. In *Ultrafast Phenomena XI*; Elsasser, T., Fujimoto, F. G., Wiersma, D. A., et al., Eds.; Springer Verlag: New York, 1998; p 623.
(48) Kaindl, R. A.; Wurm, M.; Reimann, K.; Hamm, P.; Weiner, A. M.; Woerner, M. *J. Opt. Soc. Am. B* **2000**, *17*, 2086.
(49) Ketterle, W.; Grashoff, P.; Figger, H.; Walther, H. *Z. Phys. D* **1988**, *9*, 325.
(50) Kaspar, J.; Smith, V. H., Jr.; MeMaster, B. N. *Chem. Phys*. **1985**, *96*, 81.
(51) Raynor, S.; Herschbach, D. R. *J. Phys. Chem*. **1982**, *86*, 3592.
(52) Cardy, H.; Liotard, D.; Dargelos, A.; Poquet, E. *Chem. Phys*. **1983**, *77*, 287.
(53) Park, J. K. *J. Chem. Phys.* **1997**, *107*, 6795.
(54) Park, J. K. *J. Chem. Phys.* **1998**, *109*, 9753.
(55) Freed, K. F. In *Topics in Applied Physics*; Fong, F. K., Ed.; Springer-Verlag: New York, 1976; Vol. 15.
(56) Freed, K. F.; Jortner, J. *J. Chem. Phys*. **1970**, *52*, 6272.
(57) Takasu, R.; Hashimoto, K.; Fuke, K. *Chem. Phys. Lett*. **1996**, *258*, 94.
(58) Hertel, I. V.; Huglen, C.; Nitsch, C.; Schultz, C. P. *Phys. Rev. Lett*. **1992**, *67*, 1767.
(59) Misaizu, F.; Tsukamoto, K.; Sanekata, M.; Fuke, K. *Chem. Phys. Lett*. **1992**, *188*, 241.
(60) Unterreiner, A.; Lindner, J.; Vohringer, P. In *Femtochemistry and Femtobiology: Ultrafast Dynamics in Molecular Sciences*; Douhal, A., Santamaria, J., Eds.; World Scientific: Singapore, 2002.